NASA/TM—2007–214958

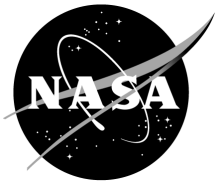

Liquid Bismuth Propellant Management System for the Very High Specific Impulse Thruster With Anode Layer

K.A. Polzin and T.E. Markusic
Marshall Space Flight Center, Marshall Space Flight Center, Alabama

B.J. Stanojev
WFI Government Services, Inc., Huntsville, Alabama

May 2007

The NASA STI Program…in Profile

Since its founding, NASA has been dedicated to the advancement of aeronautics and space science. The NASA Scientific and Technical Information (STI) Program Office plays a key part in helping NASA maintain this important role.

The NASA STI program operates under the auspices of the Agency Chief Information Officer. It collects, organizes, provides for archiving, and disseminates NASA's STI. The NASA STI program provides access to the NASA Aeronautics and Space Database and its public interface, the NASA Technical Report Server, thus providing one of the largest collections of aeronautical and space science STI in the world. Results are published in both non-NASA channels and by NASA in the NASA STI Report Series, which includes the following report types:

- TECHNICAL PUBLICATION. Reports of completed research or a major significant phase of research that present the results of NASA programs and include extensive data or theoretical analysis. Includes compilations of significant scientific and technical data and information deemed to be of continuing reference value. NASA's counterpart of peer-reviewed formal professional papers but has less stringent limitations on manuscript length and extent of graphic presentations.

- TECHNICAL MEMORANDUM. Scientific and technical findings that are preliminary or of specialized interest, e.g., quick release reports, working papers, and bibliographies that contain minimal annotation. Does not contain extensive analysis.

- CONTRACTOR REPORT. Scientific and technical findings by NASA-sponsored contractors and grantees.

- CONFERENCE PUBLICATION. Collected papers from scientific and technical conferences, symposia, seminars, or other meetings sponsored or cosponsored by NASA.

- SPECIAL PUBLICATION. Scientific, technical, or historical information from NASA programs, projects, and missions, often concerned with subjects having substantial public interest.

- TECHNICAL TRANSLATION. English-language translations of foreign scientific and technical material pertinent to NASA's mission.

Specialized services also include creating custom thesauri, building customized databases, and organizing and publishing research results.

For more information about the NASA STI program, see the following:

- Access the NASA STI program home page at <http://www.sti.nasa.gov>

- E-mail your question via the Internet to <help@sti.nasa.gov>

- Fax your question to the NASA STI Help Desk at 301–621–0134

- Phone the NASA STI Help Desk at 301–621–0390

- Write to:
  NASA STI Help Desk
  NASA Center for AeroSpace Information
  7115 Standard Drive
  Hanover, MD 21076–1320

NASA/TM—2007–214958

Liquid Bismuth Propellant Management System for the Very High Specific Impulse Thruster With Anode Layer

K.A. Polzin and T.E. Markusic
Marshall Space Flight Center, Marshall Space Flight Center, Alabama

B.J. Stanojev
WFI Government Services, Inc., Huntsville, Alabama

National Aeronautics and
Space Administration

Marshall Space Flight Center • MSFC, Alabama 35812

May 2007

Acknowledgments

We appreciate the management support of Mike Fazah and Jim Martin, and the support of Dr. Michael LaPointe in the Program Office, throughout the duration of this effort. We also acknowledge the contributions of Doug Davenport, Doug Galloway, Tommy Reid, Keith Chavers, Rondal Boutwell, and Jeff Gross to this effort. We appreciate the contributions Dr. Marrese-Reading of NASA's Jet Propulsion Laboratory made throughout the course of this project and especially acknowledge that she performed extensive testing of a complete propellant management system comprised of our hardware and her propellant vaporizer.

The Very High Specific Impulse Thruster with Anode Layer program was supported by NASA's Exploration Systems Mission Directorate (Project Prometheus) and funded under contract NAS7–03001 managed by John Warren. Partial support for this work has been provided by NASA Marshall Space Flight Center's Technology Transfer Office.

Available from:

NASA Center for AeroSpace Information
7115 Standard Drive
Hanover, MD 21076–1320
301–621–0390

This report is also available in electronic form at
<https://www2.sti.nasa.gov>

TABLE OF CONTENTS

LIST OF FIGURES

LIST OF FIGURES (Continued)

LIST OF ACRONYMS

ac	alternating current
CAD	computer-aided drafting
CF	conflat
cRIO	compact reconfigurable input/output
dc	direct current
EM	electromagnetic
EP	electric propulsion
EPR	electropneumatic regulator
FEEP	field emission electric propulsion
FPGA	field programmable gate array
HOR	hand-operated regulator
I/O	input/output
JPL	Jet Propulsion Laboratory
MPD	magnetoplasmadynamic
MSFC	Marshall Space Flight Center
NI	National Instruments
PV	pressure vessel
SCR	silicon-controlled rectifier
SOV	solenoid operating valves
TAL	thruster with anode layer
TM	Technical Memorandum
VHITAL	very high specific impulse thruster with anode layer

NOMENCLATURE

a	linear curve fit coefficient
B	magnetic field strength
E	energy
I	total current
I_{sp}	specific impulse
L	distance between heating location and sensing location; length
P	pressure
R	electrical resistance
s	channel height
T	temperature
T_B	boiling temperature
T_M	melting temperature
t	time
u	flow speed
α	thermal diffusivity
Δt	pulse duration
τ_c	thermal convection timescale
τ_d	thermal diffusion timescale

TECHNICAL MEMORANDUM

LIQUID BISMUTH PROPELLANT MANAGEMENT SYSTEM FOR THE VERY HIGH SPECIFIC IMPULSE THRUSTER WITH ANODE LAYER

1. INTRODUCTION

1.1 Motivation

Operation of Hall thrusters with bismuth propellant has been shown as a promising path for the development of high-power (140 kW per thruster), high-performance (8,000 s specific impulse (I_{sp}) at >70% efficiency), electric propulsion systems for spaceflight missions.[1] The use of bismuth also alleviates several logistical issues that would normally be associated with development and deployment of a high-power Hall thruster operating on xenon, which is the traditional propellant option. The cost of propellant for testing and performance of deep-space missions is not nearly as prohibitive since bismuth costs far less than xenon ($75/kg compared to $2,000/kg as of this writing). Also, since it is solid at room temperature, vaporized bismuth can be condensed using simple, water-cooled plates, essentially cryopumping the propellant at room temperature and obtaining equivalent pumping speeds of millions of liters per second. Finally, while xenon-fed Hall thrusters have difficulty operating at high voltages (>1 kV), thrusters using bismuth have achieved very high I_{sp} because they can operate at voltages approaching 10 kV.

The work described in this Technical Memorandum (TM) is part of the Very High I_{sp} Thruster with Anode Layer (VHITAL) program.[2] This program represented one of several domestic efforts aimed at validating the high performance of bismuth-fed Hall thrusters and understanding the physical mechanisms that allow for high-voltage, high-power, high-performance operation.[1] NASA Marshall Space Flight Center's (MSFC's) role in the VHITAL program was focused on the design, construction, and evaluation of a propellant management system that could deliver liquid bismuth to a Hall thruster while simultaneously monitoring the propellant flow rate. This was a critical element of the VHITAL program since performance cannot be accurately assessed without precise knowledge of the mass flow rate. Previous performance measurements[1] used a pretest/posttest propellant weighing scheme that did not provide any real-time measurement of the mass flow rate during thruster operation, leading to relatively large error bars on both I_{sp} and thrust efficiency. The VHITAL propellant management system was designed to obtain more accurate, temporally resolved flow rate measurements. The overall system was also designed as a test bed where hardware and control algorithms could be evaluated for future propellant feed system development efforts.

1.2 Definition of the Problem

In the VHITAL thruster, the bismuth propellant must undergo three phase transitions—solid to liquid, liquid to gas, and gas to plasma. The primary function of the propellant management system

is the delivery of gaseous propellant to the discharge chamber at a prescribed mass flow rate. This can be accomplished by any one of the three methods schematically illustrated in figure 1 and discussed below.

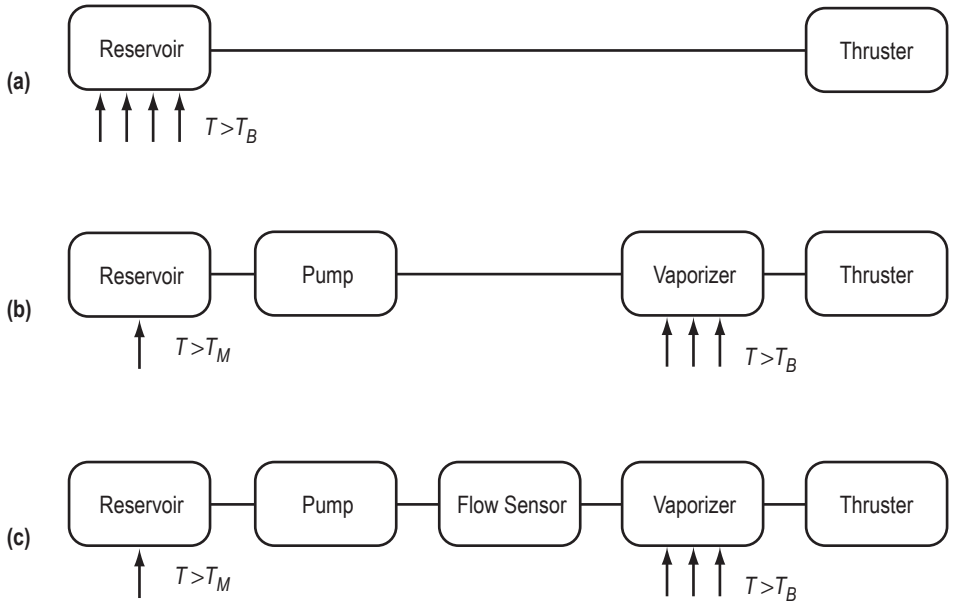

Figure 1. Simplified schematic of three increasingly complex approaches for delivering metallic propellant from a reservoir to a thruster.

In the simplest scenario, sufficient heat to both melt and vaporize the propellant is applied to the reservoir, and gas is directly delivered to the discharge chamber. This method was used in the earlier Russian bismuth thruster with anode layer (TAL) program.[1] The main appeal of this approach is its simplicity. The primary drawbacks are as follows: (1) The necessity of heating a large volume of metal to high temperature $T > T_B$ (boiling temperature) and the potential for condensation in the line between the reservoir and thruster, (2) lack of instantaneous control due to large thermal inertia, and (3) ambiguity in the instantaneous mass flow rate measurement. (No suitable flow meter exists for measuring high-temperature metallic gas flow rates.)

A second approach involves the addition of two components to the feed system—a liquid pump and a vaporizer. This configuration isolates the high-temperature components associated with vaporization to a small region immediately adjacent to the thruster, thus reducing the total high-temperature surface area (and concomitant radiative heat losses). The relatively cool liquid propellant $T > T_{\mathrm{M}}$ (melting temperature) can be pumped to the high-temperature vaporizer by one of several possible methods; e.g., gas pressurization, mechanical piston, or electromagnetic pump.[3]

The functionality of the second approach is further enhanced by the addition of an in-line liquid flow sensor, as illustrated in figure 1. In addition to providing a real-time mass flow rate measurement, the flow sensor can also be used to provide flow rate feedback to the pump component, thus enabling the implementation of a true control system and precision, real-time flow control.

A preliminary analysis allowed for the identification of the following additional bismuth-specific challenges associated with the development of the propellant management system:

- The high density of bismuth ($\mathcal{O}(10^4)$ kg/m^3) and low propellant mass flow rate ($\mathcal{O}(10^{-6}$–$10^{-5})$ kg/s) results in a very low volume flow rate ($\mathcal{O}(10^{-10}$–$10^{-9})$ m^3/s) that is challenging to continuously monitor using in-line flow sensors. The high density of the propellant also causes gravitational influences on the feed line pressure, as the propellant level in the tank recedes during testing, which must be compensated for by varying the pumping pressure.

- The high melting temperature of bismuth (≈275 °C) makes it difficult to employ many off-the-shelf components; e.g., valves and electronics. Consequently, many of the feed system components require custom design and fabrication.

- The relatively low volumetric flow rate of bismuth makes it nearly impossible to measure the flow rate electromagnetically, as was previously done for lithium.[4] Flow sensing elements that are in direct contact with the flow must be electrically insulated, but the high temperature of molten bismuth precludes the use of some of the most attractive insulators.

- The feed system and any electrical connections must be shielded from condensing bismuth vapor from the thruster exhaust as this can electrically short some of the feed system components, rendering them inoperable.

2. LITERATURE REVIEW

Since the 1960s, there have been many different electric propulsion (EP) applications in which a liquid metal has been used as the propellant source. In these various applications, the propellant is typically delivered in liquid form, either to a vaporizer operating at elevated temperature (temperature-controlled atomization) or to a vaporizer occupying a region possessing a high electric field (field ionization-controlled atomization). The following is a brief review of the different techniques that have been employed to feed liquid metals from their reservoirs to vaporizers in electric thrusters.

2.1 Passive Propellant Feeding

Liquid metal propellants can be controlled passively using surface tension and the capillary forces that naturally arise. For any wetting propellant, the capillary forces act to move the liquid metal into channels with smaller cross-sectional areas. A system of this type can be advantageous since it has no moving parts. In addition, there are no components in the system that preclude it from operation at elevated temperatures. The maximum liquid (capillary) flow and pressure head at the vaporizer are fixed in this type of system. For simple geometries, these flow parameters can be computed based upon the propellant feed system geometry and the surface tension properties of the given liquid.[5]

Surface tension-driven systems have been used quite extensively in EP. Cesium ion thrusters appear to have been the first to employ this type of propellant management system for a liquid metal.[6–8] Ion thrusters employing individual capillary channels and porous tungsten 'sponges' to 'wick' the propellant from a reservoir and transfer it to the vaporizer have both been operated. More recently, capillary forces have been used for propellant management in cesium[9] and indium[10] field emission electric propulsion (FEEP) systems.

2.2 Active Control

Variable, externally applied forces can be applied to liquid metals using a number of different techniques to exercise active control over the propellant flow rate and/or pressure force exerted by the liquid metal vaporizer plug. In EP devices, active propellant management has been accomplished using the following:

- Elastic diaphragms.
- Metallic bellows or pistons.
- Electromagnetic pumps.
- Direct propellant vaporization.

Elastic diaphragms separate the propellant reservoir into two sections—one containing the liquid metal propellant and the other initially evacuated or at low pressure. A variable and controllable force is exerted upon the propellant by increasing the gas pressure in the initially evacuated section. The gas pressure may be increased by using a pressure-regulated gas supply or by using heat to vaporize and

expand a substance that is initially solid or liquid, such as carbon dioxide or freon. In either case, the pressure increases and propellant is displaced from the reservoir and pushed into the feed lines toward the thruster. This technique works well for propellants like mercury where the temperature levels in the reservoir are not too high. However, the diaphragm can melt if this technique is attempted for a propellant with a high melting point like bismuth or lithium.

Conceptually, metallic bellows and pistons operate in much the same way as the elastic diaphragms. The bellows form a propellant reservoir that decreases in size as the bellows are contracted. This contraction forces the propellant out of the reservoir and toward the thruster. Pistons are driven using electric motors and simply contract the space by advancing into the propellant tank. These approaches work for high-temperature liquid metal propellants, but there is a mass associated with the use of motors. Also, the reservoir volume change occurs in a series of 'steps' instead of a smooth, continuous transition.

Electromagnetic (EM) pumps exploit the fact that liquid metals are conducting fluids capable of carrying current. By orienting an applied magnetic field perpendicular to a current passing through the liquid metal, a $\mathbf{j}\times\mathbf{B}$ Lorentz body force is exerted on the fluid. This can have the effect of either accelerating the propellant as it passes through the EM pump or increasing the pressure head the fluid exerts at the thruster vaporizer. Electromagnetic pumps can operate at elevated temperatures, but temperature limits can be reached, especially if the applied magnetic field is produced using permanent magnets.

Finally, propellant can be vaporized in the reservoir and then allowed to migrate toward the thruster. This method is simple and robust, owing to the lack of mechanical components in the system. It is considered active in that there can be no propellant mass flow without the external application of heat. However, this technique does not offer a high degree of controllability in the mass flow rate and is not readily amenable to mass flow rate measurements. This makes it difficult to accurately compute thruster performance.

Elastic diaphragms appear in the EP literature in conjunction with mercury ion engines.[11–13] Unlike in the cesium ion engines previously discussed, mercury is a nonwetting fluid. Consequently, it must be actively forced out of the propellant reservoir toward the thruster.

Propellant management systems using metallic bellows or pistons typically appear in the literature for thrusters operating on liquid lithium. The bellows system was employed during the 1960s on a magnetoplasmadynamic (MPD) arcjet.[14,15] More recently, a piston-controlled lithium feed system has been operated in conjunction with a Lorentz force accelerator.[16,17]

Electromagnetic pumps have not been operated in a thruster as the primary propellant feeding mechanism. They have, however, been used in conjunction with elastic diaphragm systems in mercury ion engines.[11–13] In these systems, the EM pump acted as a mechanism to provide fine adjustment of the mercury pressure head at the vaporizer. One such pump[12] produced a pressure differential of 0.6 atm when operating at a current level of 20 A.

In recent thruster experiments, the direct vaporization technique has been used to feed propellant from a propellant reservoir to a thrust chamber. This feed technique was employed on a bismuth-fed,

TAL-type Hall thruster.[1] More recently, a lithium Lorentz force accelerator employed an open-ended heat pipe design to vaporize and directly feed gaseous propellant to the thruster.[18]

2.3 Current State of the Art

Several of the liquid metal feed systems previously described have reached an advanced state of readiness. Capillary-fed cesium ion thrusters and FEEP systems have either achieved flight-ready status or have successfully flown in space. Also, mercury ion engines employing elastic diaphragms have flown on such missions as SERT 1 and 2. Unfortunately, the nonwetting characteristics of liquid bismuth preclude us from using the capillary feed mechanism while bismuth's high melting point eliminates the possibility of using an elastic diaphragm.

The piston-driven propellant management system[16,17] currently represents the state of the art for controlling a hot liquid metal propellant like bismuth or lithium (fig. 2). Propellant mass flow rate can be measured by computing the propellant tank volume that the piston sweeps out over a given time. This technology is still at the research level of readiness.

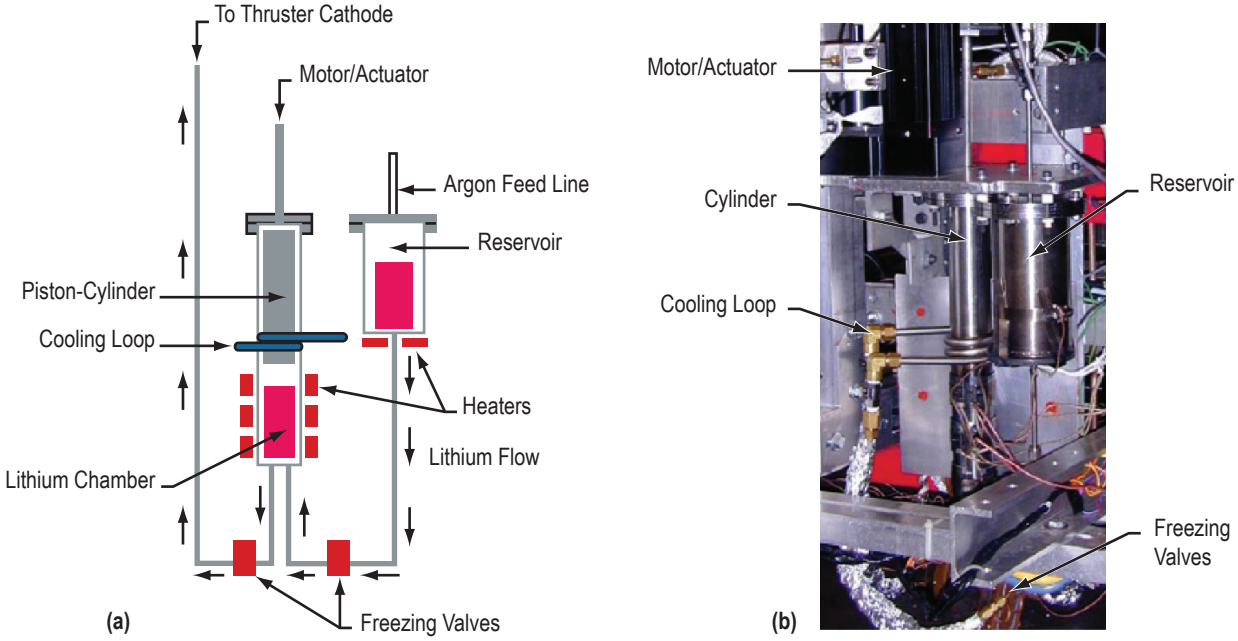

Figure 2. Princeton piston-driven lithium feed system: (a) Schematic and (b) photograph (from ref. 16).

Electromagnetic pump technology[11–13] may also be considered at or near the current state of the art. This technology has the advantage of possessing no moving parts. In the thruster application, the technology readiness level is slightly below the piston-driven system as EM pumps have not been used as the primary control component in a propellant management system and have not been used in conjunction with high-temperature liquid metal flows on the small scale being considered for the VHITAL research project. They have, however, flown in space as the primary flow control component for the much higher flow rate SNAP 10A nuclear reactor.[19]

3. VERY HIGH SPECIFIC IMPULSE THRUSTER WITH ANODE LAYER PROPELLANT MANAGEMENT SYSTEM

The VHITAL propellant management system consists of two separate subsystems:

(1) The feed system encompasses the components that are located in near proximity to the thruster. These are the components that are designed to operate in a vacuum chamber; many are in direct physical contact with liquid bismuth.

(2) The control system is remotely located, containing a computer control interface, specialized circuitry for flow sensor operation, and power supplies for actuation of the feed system components.

3.1 Feed System Hardware

Two separate feed systems were developed for the VHITAL project. These were both designed to tackle the difficulties listed in section 1.2.

The first was a simple gas pressure-driven system (fig. 3) that was constructed primarily using off-the-shelf components to enable immediate experimental testing of bismuth vaporizers at NASA's Jet Propulsion Laboratory (JPL). This system operates by first heating a bismuth reservoir to a temperature above the melting point of bismuth. Argon gas pressure is then introduced into the reservoir to force the bismuth through a feed tube toward the vaporizer. The pressure-driven system is subsumed in the second, more complex system, and will only be discussed in passing throughout the rest of this TM.

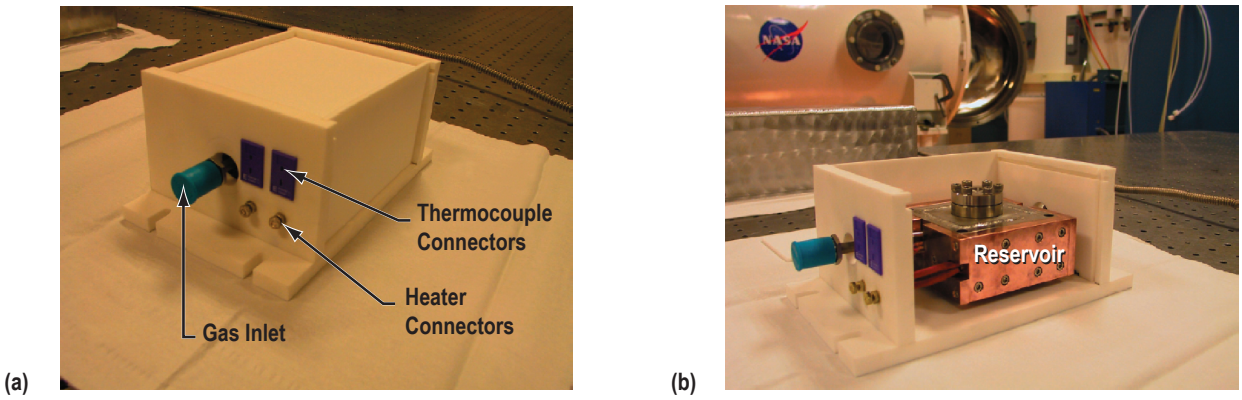

Figure 3. Photographs of VHITAL pressure-driven reservoir assembly: (a) With heat shield panels and (b) with two of the heat shield panels removed.

The second system includes more components than the first system and operates in the following manner. A propellant reservoir containing solid bismuth is heated until its temperature is above

bismuth's melting temperature. The liquid bismuth can be made to move using a combination of two different techniques. The application of gas pressure to the reservoir forces molten bismuth through the system. The second method, which exploits the fact that bismuth is an electrically conducting fluid, employs an EM pump that is integrated into the propellant feed line downstream of the reservoir. An in-line flow sensor capable of making real-time measurements completes the propellant feed system. The entire system is shown in figure 4. Each of these four major components is discussed in greater detail in sections 3.1.1 through 3.1.4.

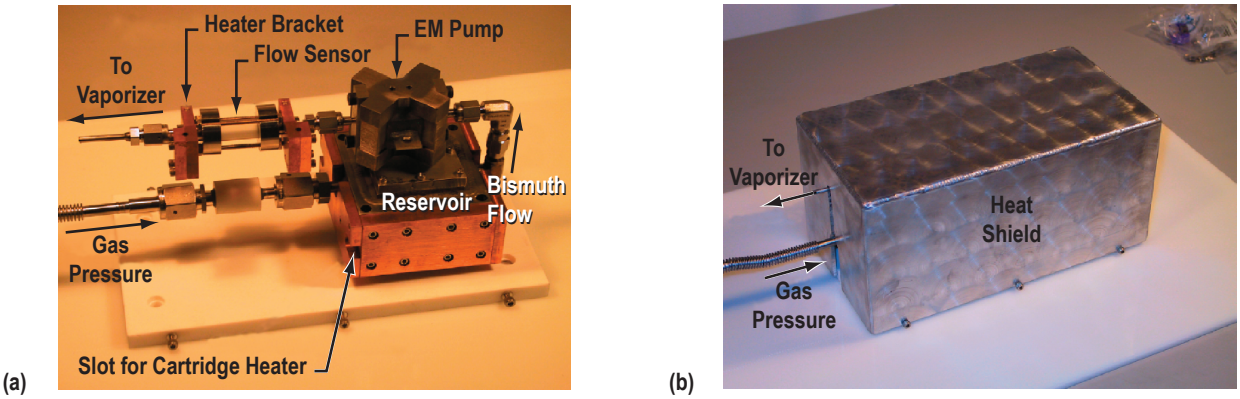

Figure 4. Assembled bismuth propellant feed system: (a) Without heat shield cover and (b) with heat shield cover installed.

3.1.1 Propellant Reservoir

The reservoir is designed to allow for the storage and melting of high-purity bismuth. It is fabricated from 316L stainless steel and has a removable lid for loading bismuth. An inlet tube welded into the body allows for gas pressurization that forces liquid bismuth out of the reservoir through an outlet tube. Two 3-in-long, ¼-in-diameter Watlow cartridge heaters are operated between 45 and 80 W total input power to heat the reservoir. Copper plates bolted to the steel structure are employed to uniformly distribute heat to the reservoir. The reservoir lid was initially sealed using a conflat (CF) copper gasket flange in the pressure-driven system. In the second system, a Parker metal C-ring was employed to seal the reservoir. However, over the course of several thermal cycles, it was found that both the CF flange and the C-ring seal lost their effectiveness. The C-ring especially lost its elasticity during testing. The final system employed Grafoil® to form a seal between the reservoir and the lid.

3.1.2 Gas Pressurization System

The gas pressurization system (fig. 5) is designed to provide gas pressurization to the reservoir within the (continuously adjustable) range of zero to 200 torr. The system is designed to operate inside a vacuum chamber, allowing for ease of integration with other thruster subsystems.

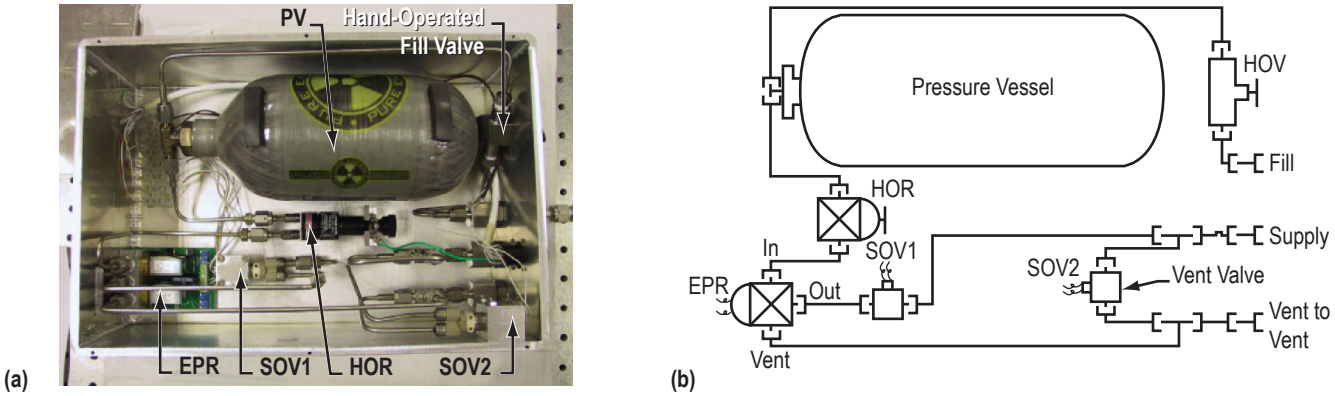

Figure 5. Gas pressurization system: (a) Photograph and (b) schematic representation.

The pressure vessel (PV) is a 0.7-L, fiber-wound cylinder rated to 4,500 psi. The hand-operated regulator, which reduces the high pressure in the reservoir to the lower pressure required for the electropneumatic regulator (EPR) actually limits the pressure rating of the system to roughly 200 psi. The hand-operated regulator is designed for "low-bleed" applications where the volume flow rate is expected to be small, as is the case in the VHITAL reservoir. Two solenoid-operated valves (SOV1 and SOV2) are used to isolate the propellant reservoir from the gas pressurization system and vent the pressurized lines directly to vacuum. The hand-operated valve—a Swagelok ball valve—connects the 'fill' port on the front panel to the PV. It is used to allow repeated pressurization (filling) of the PV.

The Marsh-Bellofram EPR is the heart of the gas pressurization system, using a 'bang-bang' arrangement of solenoid valves. The propellant reservoir pressure is set to the desired value by alternately opening and closing the high pressure and vacuum valves. An onboard control system uses a feedback signal from an onboard pressure transducer to determine the proper sequencing of the SOV open/close operations. External control is maintained using a zero to 10 Vdc signal that allows for continuous, remote adjustment of the reservoir gas pressure.

3.1.3 Electromagnetic Pump

An EM pump is incorporated in the VHITAL propellant feed system to provide an additional level of flow control. For a dc conduction pump with a magnetic field (B) and a total current (I), it can easily be shown[20] that the pressure change induced in a conducting fluid is equal to

$$\Delta P = \frac{I\,B}{s}\,, \tag{1}$$

where s is the channel dimension along the applied magnetic field. Observe that the pump pressure change is only a function of the total current, total magnetic field strength, and channel height. For a fixed pump design employing permanent magnets, control is exercised by adjusting the pump current. In practice, the maximum value of B/s that can be achieved is $\mathcal{O}(10)$ T/cm.

A glass-mica ceramic (also known as Macor®) was used in the construction of the main body of the EM pump because it is stable and nonreactive with liquid bismuth near 300 °C. It is also inexpensive and easily machinable compared to other ceramics. The ease of fabrication afforded by the use of Macor versus, for example, aluminum nitride allowed for the pursuit of an aggressive design for the EM pump. Samarium cobalt magnets are employed, with a magnet separation of 2.9 mm and a channel height (s) of 2 mm. This results in an on-axis magnetic field strength (B) of 0.64 T and gives $B/s = 3.2$ T/cm.

The major components of the bismuth EM pump are shown in figure 6. The CAD model is included to show a sectioned view that reveals the inner construction. The materials used to fabricate the pump are: Macor (pump body), iron (magnet yoke), 316L stainless steel (end caps and feed lines), Inconel® (electrodes), and samarium cobalt (magnets). The electrodes are bonded to the Macor body using high-temperature epoxy and the feed lines are welded to the end caps.

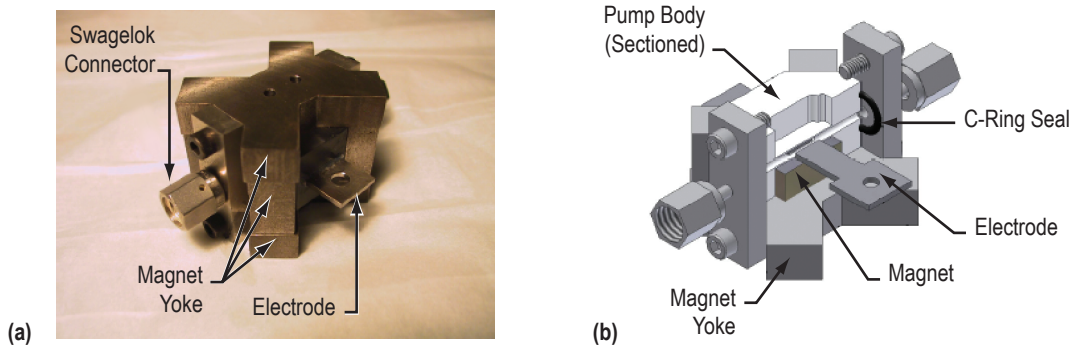

Figure 6. Electromagnetic pump: (a) Photograph and (b) CAD drawing of interior.

3.1.4 Flow Sensor

A new type of flow sensor—the hot spot flow sensor—was developed as part of this effort. The principle of operation of the device is illustrated in figure 7(a). A pulse of thermal energy (derived from a current pulse and associated joule heating) is applied near the inlet of the sensor. The flow is tagged with a thermal feature that is convected downstream by the flowing liquid metal. A downstream thermocouple records a ripple in the local temperature associated with the passing hot spot in the propellant. By measuring the time between the upstream generation and downstream detection of the thermal feature, the flow speed can be calculated using a time-of-flight analysis. This sequence of events is illustrated in figure 7(b). The spatial temperature distributions at two different times, t_0 and t_1, are conceptually illustrated. At time t_0, current is pulsed through the liquid and the temperature at the heating location locally spikes; the temperature at the thermocouple location remains at the constant, equilibrium value. At some later time t_1, the thermal feature that was created at time t_0 reaches the thermocouple and a spike in the temperature profile is observed. This spike will be somewhat smaller in peak temperature and broader in spatial extent because the thermal feature will diffuse as it is convected downstream.

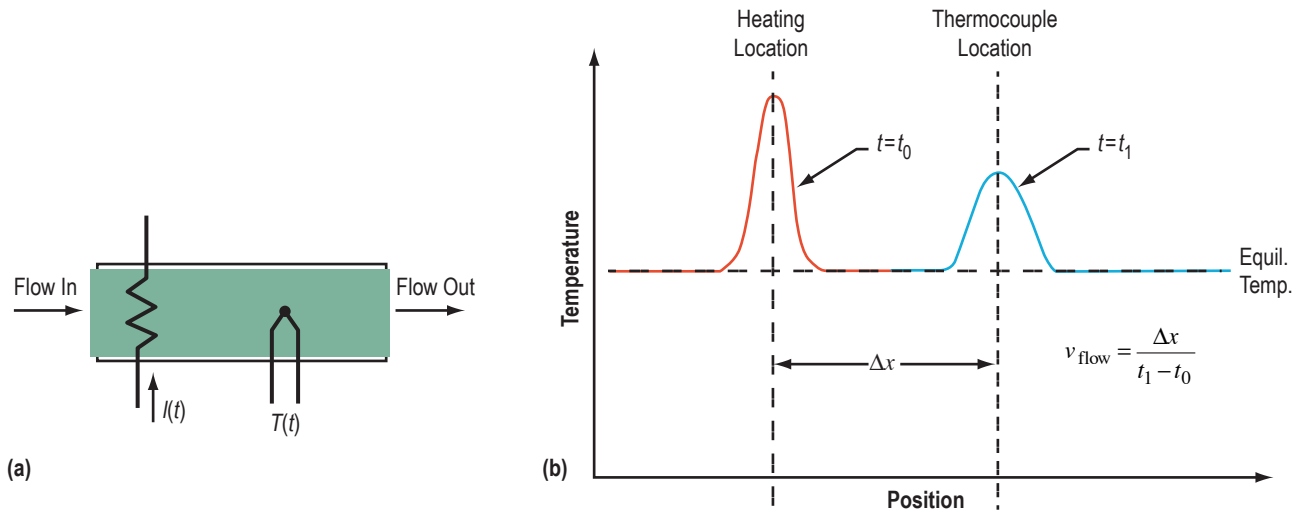

Figure 7. Hot spot flow sensor: (a) Schematic illustrating the principle of operation and (b) illustration of the temporal evolution of the temperature distribution in the flow sensor.

The primary advantage of this technique is that it does not depend on an absolute measurement of temperature but, instead, relies on the observation of thermal features. This makes the technique insensitive to other externally generated, low-frequency thermal fluctuations. The hot spot in the upstream flow is generated by pulsing current directly through the liquid metal; doing so exploits the intrinsic resistivity of the fluid and obviates the need for a separate resistive heating element. In order for the hot spot flow sensor to provide useful results, the spatial integrity of the hot spot must be maintained until it reaches the thermocouple location. The hot spot will tend to flatten out as it propagates, due to thermal diffusion. Therefore, the device must be designed such that the thermal diffusion timescale is much larger than the convective timescale.

The energy required to locally elevate the temperature to a given value above the inlet temperature can be estimated if the resistive heating is assumed to occur instantaneously at time t_0. A temperature change of $\mathcal{O}(1)$ °C is readily measurable. Since the peak temperature will decay as the thermal feature propagates, the flow should initially be heated to $\mathcal{O}(10)$ °C to ensure that the feature can be detected downstream. If the flow channel is $\mathcal{O}(1)$ mm diameter, and the axial extent of the heated region is assumed as $\mathcal{O}(1)$ mm, the energy input required to locally raise the temperature $\mathcal{O}(10)$ °C is $\mathcal{O}(10)$ mJ. In practice, the energy required to create the hot spot is much greater due to resistive losses in the external current pulse circuit. The electrical resistance of the hot spot is small because the flow sensor channel diameter is small ($\mathcal{O}(1)$ mΩ in the case of bismuth). Consequently, external circuit series resistance losses dominate the system, making it impossible to determine the actual energy requirement without a complete description of the external circuit. The current level required to generate the hot spot can be estimated assuming resistive heating of the flow and a flat-top current pulse:

$$I = \left(E \big/ R\, \Delta t \right)^{1/2} , \tag{2}$$

where I is the current, E is the energy required to locally heat the flow 10 °C, and Δt is the pulse duration. Using the characteristic order of magnitude estimates given above, and assuming a pulse width of $\mathcal{O}(100)$ μs, the required current level is $\mathcal{O}(100)$ A, which is easily accessible using capacitively stored energy and standard solid state switches.

The spatial integrity of the hot spot must be maintained as it propagates between the heating and sensing locations so that the time of flight between the two locations can be accurately determined. This implies that the convection timescale should be small compared to the diffusion timescale. The convection timescale is the ratio of the characteristic device length (distance between the heating location and sensing location (L)) to the characteristic flow speed (u):

$$\tau_c = L/u \quad . \tag{3}$$

The diffusion timescale is governed by the material properties (the thermal diffusivity (α)) and the characteristic length of a temperature gradient which, in the present case, is the characteristic device length (L):

$$\tau_d = L^2/\alpha \quad . \tag{4}$$

Consequently, to ensure integrity of the hot spot at the sense location, the device must be constructed such that

$$\tau_c/\tau_d = \alpha/L\,u < 1 \quad . \tag{5}$$

Typical device dimensions are $\mathcal{O}(1)$ cm, so the channel diameter must be sized to assure that the flow speed is sufficient to make $\tau_c/\tau_d < 1$. Also, it is clear that the device will work best with low α liquids, such as bismuth.

As with the pump, the flow sensor is constructed around a Macor central body (fig. 8). The fluid connectors at the ends of the sensor and the heating electrodes are fabricated from 316L stainless steel. The downstream temperature measurement is acquired using a 0.002-in-diameter butt-welded type E thermocouple that penetrates the Macor body, with ≈1-cm axial separation from the heating location. The electrodes and thermocouples are bonded to the Macor body using a high-temperature epoxy. The flow channel has a diameter of 0.022 in, which results in a bismuth flow speed of ≈0.5 cm/s at a mass flow rate of ≈10 mg/s.

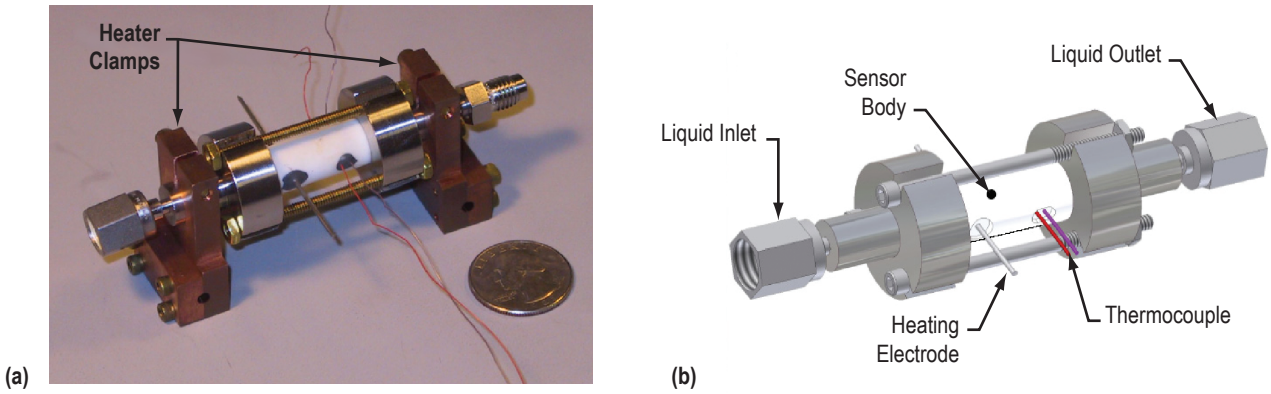

Figure 8. Assembled hot spot flow sensor assembly: (a) Photograph and (b) CAD drawing.

3.1.5 Component Connections

The components comprising the VHITAL feed system are connected using Swagelok VCR fittings. Since bismuth appears to attack or alloy with copper and nickel, all the VCR fittings that are exposed to molten bismuth are sealed using unplated stainless steel gaskets. In addition, the tubing carrying bismuth is all composed of 316L stainless steel to resist corrosion. Finally, the connections at the EM pump and flow sensor Macor-stainless steel interfaces are compression sealed using Parker unplated Inconel C-rings.

3.1.6 Additional Heating

Additional heat is added to the system at the ends of the flow sensor (fig. 4) and the EM pump (not shown in the figure). At the ends of each component, a copper heater bracket is clamped onto the stainless steel endcaps that compress the metal C-ring seal. Heating the ends of the ceramic components in this manner helps ensure that the molten bismuth will not freeze once it reaches the pump or flow sensor. One small Watlow cartridge heater (1 in long, $^1/_8$ in diameter) is used in each heater bracket (four total), and the heaters are all electrically connected in parallel with the power supply.

3.1.7 Thermal Isolation

The entire system containing liquid bismuth is thermally isolated from its surroundings for two reasons: (1) To help protect any surrounding equipment that may not be able to withstand the elevated temperatures and (2) to maintain a heightened temperature throughout the system, which will help keep bismuth liquid. The reservoir sits on four ¼-in Macor posts, which lift it off the base plate, also constructed of Macor, and provide little in the way of a thermal conduction path. The gas pressurization system is connected to the reservoir through a thermal isolator, also constructed of Macor, and shown in figure 4 just below the flow sensor. The tubing is wrapped in aluminum foil to help reflect any radiated heat back into the system, and the entire system is enclosed in an aluminum box, which serves the same purpose.

3.2 Control System

The VHITAL propellant management control system must not only control all the components described in the previous section but must also perform all the data sampling tasks required during operation of the feed system. Tasks include operation, adjustment, and switching of the various power supplies connected to the experiment, monitoring of any analog voltages generated by components in the system, operation of the hot spot flow sensor circuitry, and performance of temperature measurements to monitor the overall state of the feed system. This last task is made more difficult by the need to sample the flow sensor thermocouple temperature as quickly as possible to achieve an accurate measure of the flow rate.

The electronics suite developed for the VHITAL feed system (fig. 9) is centered on a National Instruments' compact reconfigurable input/output (cRIO) real-time embedded control system. This system performs all communications and data sampling required for feed system operation. The entire system has been tested in conjunction with the feed system hardware, performing within the expected parameters.

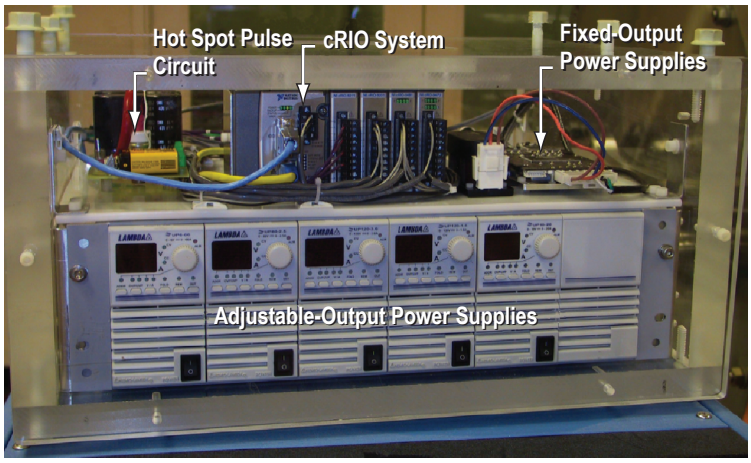

Figure 9. Control system electronics suite for the VHITAL feed system.

3.2.1 System Architecture

In general, the embedded control system can be operated as either a stand-alone system or in conjunction with an external computer. The latter mode of operation is the one implemented in the VHITAL system. In this mode, the embedded controller is passive and receives all commands from the external computer, in this case, connected using a fiber optic network converter for electrical isolation. The controller executes all the commands it receives and simultaneously monitors the feed system using if/else logic to prevent hardware damage. A schematic showing the top-level control system architecture and the flow of command and data signals between the various components is shown in figure 10.

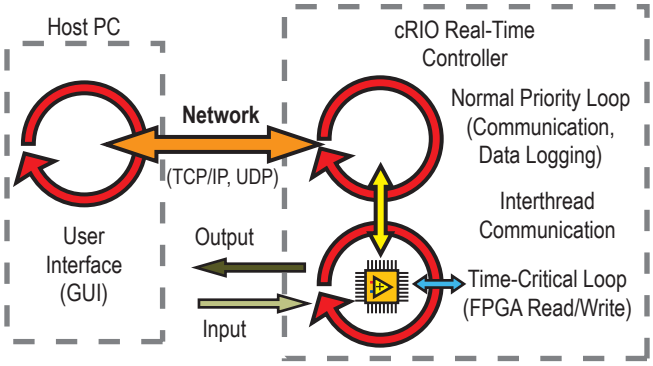

Figure 10. Control system architecture and data flow (from ni.com).

The user interface was designed in LabVIEW™ (National Instruments) and is used both to issue commands to the embedded controller and to display data from the control and data acquisition systems in real time. In principle, any standard computer with networking capability can operate as the user interface machine. The embedded controller hardware combines small format PC capabilities with a fast field programmable gate array (FPGA). The cRIO system is designed for rapid prototyping and fast signal conditioning operation using the FPGA clock for data acquisition. This system was selected for the VHITAL application because of the compact size of the cRIO unit. The particular I/O modules used were:

- NI cRIO-9002: Real-time controller with 32 MB DRAM, 64 MB compact flash.
- NI cRIO-9201: 8-channel, ±10 V, 500 kS/s, 12-bit analog input module.
- NI cRIO-9481: 4-channel, sourcing digital output single-pole, single-throw relay module.
- NI cRIO-9472: 8-channel, 24 V logic, 100 µs, sourcing digital output module.
- NI cRIO-9211: 4-channel, 14 sample/s, 24-bit, ±80 mV thermocouple input module.

3.2.2 Power Supplies

The control system uses two separate power subsystems. A Vicor dual output ac/dc converter is used to provide power to the electronics. These include the cRIO module, optical network converter, and cooling fan. In addition, this supply is switched using the cRIO-9481 module to energize the solenoid valves SOV1 and SOV2 in the gas pressurization system. Five variable Lambda ZUP output power supplies are used to provide adjustable power to the feed system. These supplies were selected because they have a small form factor, are easily packaged into a cluster, and can be controlled through a serial connection. The supplies are interconnected and adjusted by the real-time controller using the RS-485 communication protocol. The supplies monitor their current and voltage outputs and send these data back to the controller using the same communications protocol. The following is a list of the specifications and primary function of each power supply:

- Magnetic pump: 6 V/66 A (≈5 W).
- Component cartridge heaters: 80 V/2.5 A (10–45 W).
- Reservoir cartridge heaters: 120 V/3.6 A (45–80 W).
- Flow sensor capacitor charge: 120 V/1.8 A.
- Gas pressure regulator control signal: 10 V/20 A (up to 0.2 W).

3.2.3 Flow Sensor Pulse Circuitry

The hot spot pulse circuitry is designed to store energy in capacitors and then release that energy in a fast pulse to thermally tag the liquid bismuth flowing between the electrodes in the flow sensor through ohmic heating. Measurements of the temperature in the flow are obtained using a thermocouple connected to the cRIO-9211 module. The flow rate is calculated by taking the time difference between the initiation of the heating pulse and the detection of the temperature 'peak' as it is convected downstream.

In the pulse circuit shown in figure 11, a silicon-controlled rectifier (SCR) (type C150 in the schematic) is used to switch the energy from the capacitor bank (1.88 mF total capacitance) into the flow sensor. The SCR is optically isolated from the control system through an optocoupler (type LL014N in the schematic), thus minimizing the risk of exposing high current to the controller. The embedded controller initiates a current pulse by triggering the SCR gate through the optocoupler. To stop current from flowing, the charge power supply is commanded to output zero volts. This drops the leakage current below the 'keep-alive' threshold of the SCR, allowing the solid state switch to open. While this active shutdown provides total isolation between the charge circuit and the real-time controller, it is also a relatively slow process.

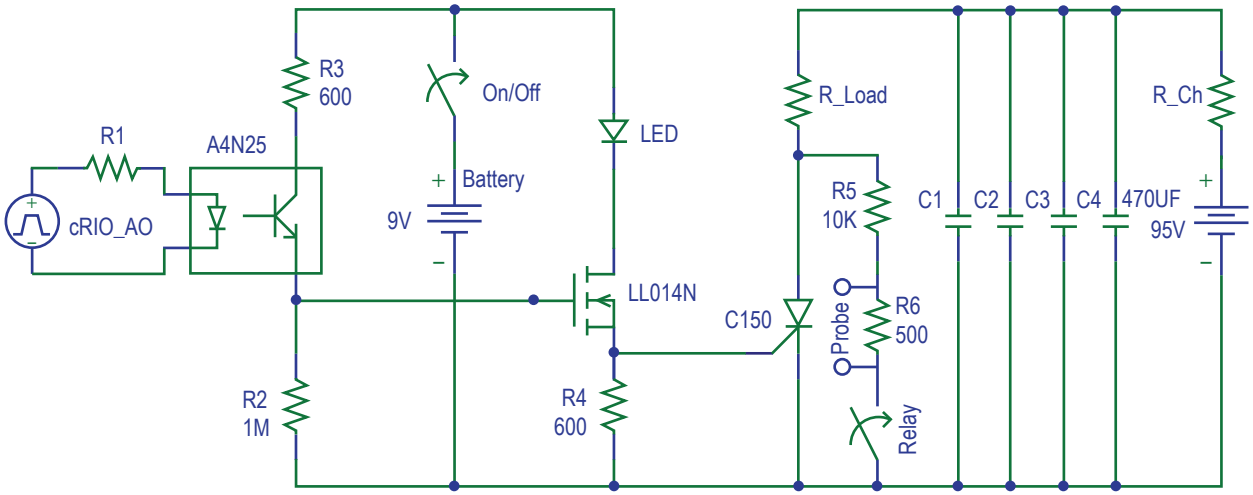

Figure 11. Schematic for the hot spot pulse circuitry. The flow sensor is denoted as R_Load and capacitors C1–C4 have a capacitance of 470 µF.

3.3 Operation

The first step in operation of the system is to melt the solid bismuth in the reservoir. This is accomplished by adding heat using the reservoir cartridge heaters. Typically, anywhere from 45 to 80 W can be used, depending on the desired rate of heating. It has been found that bismuth tends to flow more easily at reservoir temperatures in the 350 °C range. This temperature measurement is obtained from a thermocouple mounted on the outer bottom side of the reservoir.

The heaters attached to the EM pump and flow sensor endcaps are typically activated at the same time the reservoir is being heated. These heaters are operated from 10 to 45 W, and serve to bring the temperature of the components to between 300 and 325 °C. The temperature measurements for the pump and flow sensor are taken on the heated endcaps located on the downstream end of the components, so the temperatures inside the ceramic components are most certainly cooler than the thermocouples indicate.

Once the system reaches its operating temperature, gas pressure is introduced into the reservoir to force bismuth into the rest of the system. Pressure levels from 40 to 60 torr have typically proven adequate to force the bismuth up and into the pump and flow sensor. If testing is halted for some reason, the pressure is reset to zero torr so that the bismuth in the lines will resettle back into the reservoir.

When bismuth reaches the EM pump and fills the gap between the two electrodes, current may be driven to increase the pressure head in the fluid. The flow sensor can be operated when bismuth fills the gap between the electrodes. The current pulse resistively heats the fluid, and the thermal feature is detected downstream by a thermocouple inserted into the flow. The current is switched using an SCR and the amount of heating can be adjusted by changing the charge voltage applied to the pulse capacitors.

The system is shut down by first halting operation of both the flow sensor and EM pump and then venting the reservoir to vacuum. This should help bismuth recede back into the reservoir, making it easier to heat the system in subsequent tests. Finally, the heaters are turned off and the system is allowed to cool. To keep from oxidizing the tubing and bismuth propellant, it is essential that the system is allowed to cool below 100 °C before exposing it to air at atmospheric pressure.

3.4 Graphical Interface

The LabVIEW graphical interface developed to operate the feed system is pictured in figure 12. It is used to control the EPR output pressure, activate the solenoid-operated valves, adjust the heater power input to the reservoir and bismuth feed line, set the value of current passing through the EM pump, and select the length of the data sample acquired when the hot spot sensor is triggered. The interface also displays the status of these individual components as the system is operated. This includes showing the temperature as measured by several thermocouples throughout the system and displaying the pressure output measured by the EPR's onboard pressure transducer. Most importantly, though, is that the temperature data set acquired when the hot spot sensor has been pulsed is displayed in graphical form, allowing for the user to determine in real time if the sensor is operating properly.

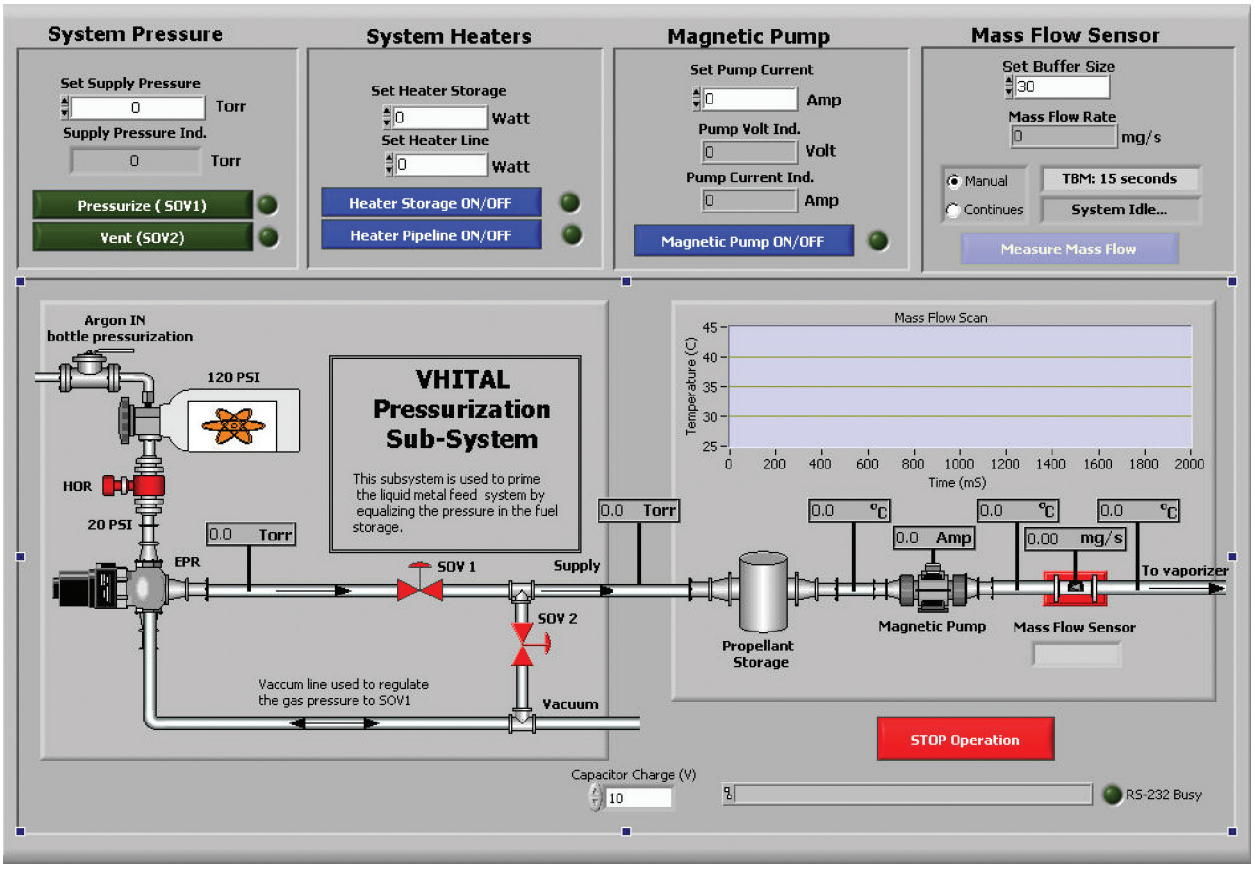

Figure 12. LabVIEW graphical interface used to control the bismuth propellant feed system.

4. SYSTEM AND COMPONENT PERFORMANCE

The entire system was tested at JPL in conjunction with a propellant vaporizer. Once primed, the pump operated successfully and current pulses were driven between the electrodes in the hot spot sensor. The flow sensing concept has been validated by acquiring hot spot flow sensor data using hot (>300 °C), flowing bismuth. To date, limited data have been acquired: additional development testing will be required to verify that the system can produce repeatable results. Postinspection of the pump and flow sensor revealed no cracking of the Macor components. Tests that quantified the performance of the gas pressurization system, EM pump, and flow sensor are detailed below.

4.1 Gas Pressurization System

The gas pressurization system was calibrated to determine the functional relationship between the command voltage and the outlet pressure. In addition, the output voltage (feedback signal from the EPR) was correlated with measured outlet pressure to allow for in situ pressure monitoring.

Calibration was accomplished by first pressurizing the PV to 150 psi with argon. The system was then placed in a vacuum chamber, and evacuated to $\approx 10^{-5}$ torr. The outlet pressure from the gas pressurization system was monitored using a Baratron® capacitance manometer.

Two calibration curves are shown in figure 13. Figure 13(a) shows the measured outlet pressure resulting from a given input voltage (command signal) and figure 13(b) shows the corresponding output voltage from the EPR onboard pressure sensor plotted against the measured outlet pressure. Resulting linear curve fits are displayed on the graphs along with the fit coefficients and associated uncertainties.

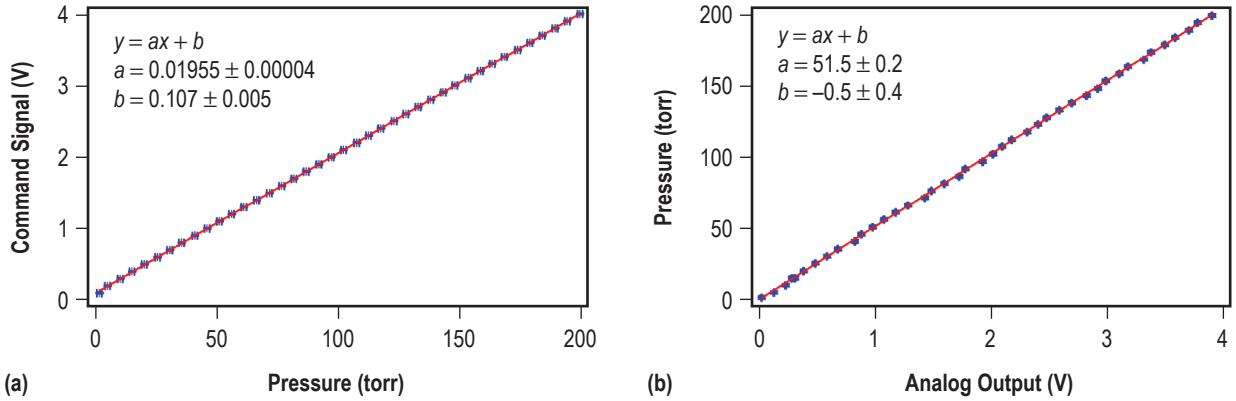

Figure 13. Gas pressure control system calibration data: (a) Command signal voltage versus measured outlet pressure and (b) measured outlet pressure versus EPR output voltage.

The complete gas-pressurized feed system was tested to verify functionality. Approximately 100 g of solid, pelletized bismuth was loaded in the reservoir and the entire apparatus was placed in a vacuum chamber. The reservoir was heated to ≈350 °C and pressurized to ≈20 torr. Liquid bismuth was expelled from the reservoir onto a sheet of stainless steel foil (fig. 14), thus demonstrating functionality of the complete gas-pressurized feed system.

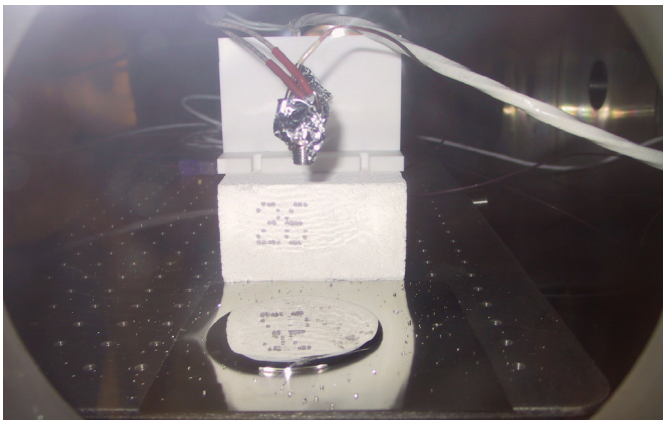

Figure 14. Liquid bismuth expelled onto a stainless steel sheet by the gas-pressurized feed system.

4.2 Electromagnetic Pump Pressure

A test apparatus was constructed to facilitate direct, quantitative measurement of the EM pump pressure as a function of applied current. In order to eliminate the difficulties associated with handling hot, liquid bismuth, these tests were conducted using a substitute liquid metal—gallium. Since the pressure developed by an EM pump is independent of the particular properties of the liquid (eq. (1)), the results of the pressure tests are generally valid for any conducting fluid, including bismuth.

The most obvious way to measure the fluid pressure drop across an EM pump is to use the pump to displace fluid inside a closed container (of fixed volume) which also contains a cover gas. Displacement of the fluid changes the gas volume inside the container and the concomitant gas pressure change can be accurately measured using a gas pressure transducer, allowing for the computation of the induced EM pump pressure. Unfortunately, at the low pressure ranges of interest, the pressure drop associated with the vertical displacement (against gravity) of a dense fluid can be comparable to the change in gas pressure. Typically, an accurate measurement of induced pump pressure can only be obtained by measuring the change in height of the fluid with high precision. To avoid the necessity of measuring both pressure and fluid height, an EM pump pressure measurement scheme using two reservoirs was employed. This approach requires simultaneous measurement of gas pressure in the two reservoirs, but eliminates the need to measure the fluid column height.

A schematic illustration of the principle of operation of the EM pump pressure measurement apparatus is shown in figure 15. The bottoms of two reservoirs are connected by an EM pump. Both reservoirs are partially filled with an electrically conducting fluid. The pressure in each (sealed) reservoir

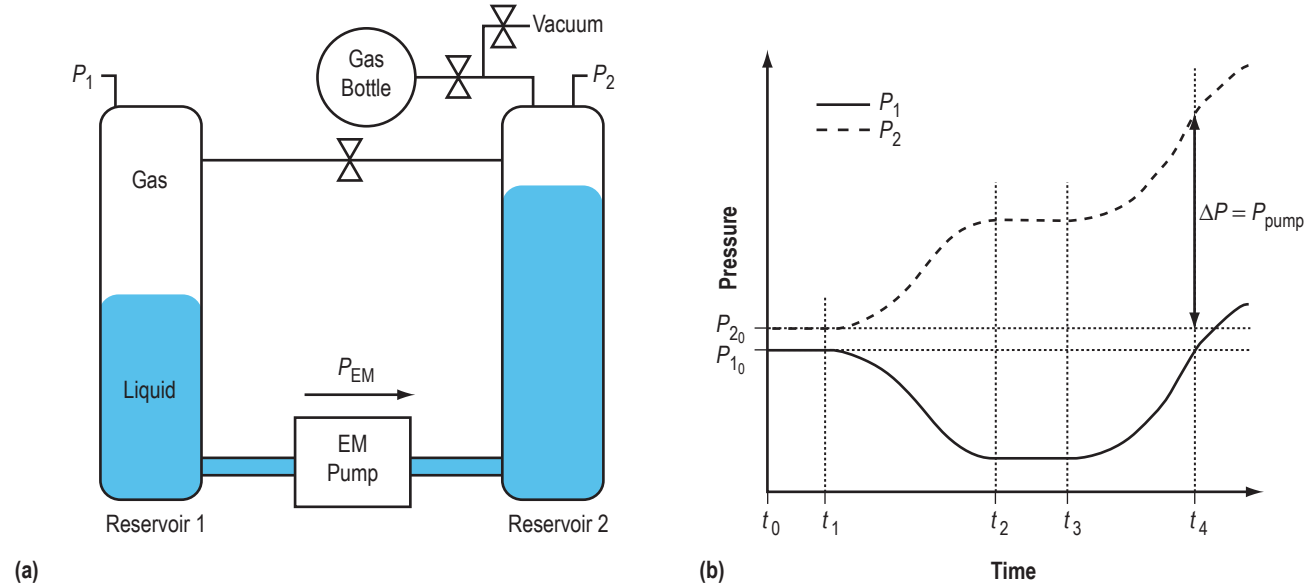

Figure 15. Schematic illustrations of EM pump pressure measurement methodology: (a) Schematic of test apparatus components and (b) notional plot of hypothetical experimental data.

is measured using a pressure transducer. The pressure in the second reservoir can be controlled by opening a valve between reservoir 2 and a high-pressure gas bottle.

The progression of events required to measure the EM pump pressure is illustrated by a hypothetical example in figure 15(b). Initially (time t_0), the fluid in each reservoir rests at its equilibrium position with the initial gas pressure in each reservoir being P_{1_0} and P_{2_0}, respectively. At time t_1 a fixed, steady current is applied to the EM pump and fluid begins to flow from reservoir 1 into reservoir 2. As fluid flows out of reservoir 1, the gas volume increases and the pressure decreases, the opposite effect occurring in reservoir 2. At some time t_2, the system reaches a new equilibrium and fluid flow ceases. If at a later time t_3, a gas valve is opened to increase the pressure in reservoir 2, the fluid will be forced from reservoir 2 back into reservoir 1. At some later time t_4, enough fluid will have been forced back into reservoir 1 to return its cover gas to its initial pressure ($P_{1_4} = P_{1_0}$), at which point the fluid levels in each reservoir will have returned to their initial equilibrium positions. When the fluid column heights return to their initial states, the excess pressure in reservoir 2 is solely balanced by the pressure applied by the EM pump:

$$\Delta P = P_{2_4} - P_{2_0} \ . \tag{6}$$

A test apparatus was constructed (fig. 16) to implement the EM pump pressure measurement strategy described above. A pressure equalization valve and a vacuum interface (also illustrated in fig. 15(a)), were included to provide flexibility in setting the initial test conditions. The pressure equalizing valve connected the tops of the two reservoirs and allowed the same initial pressure to be established in both reservoirs; i.e., $P_{1_0} = P_{2_0}$. The vacuum interface allowed for evacuation of the system to

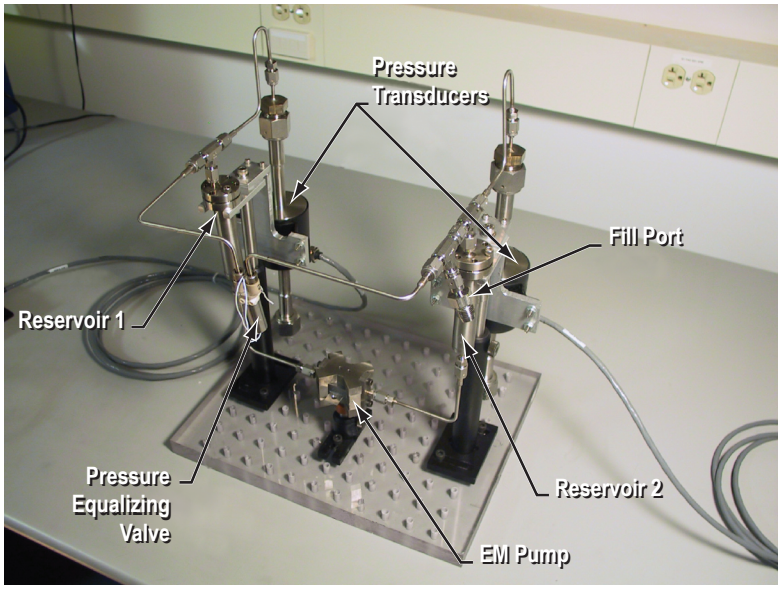

Figure 16. Electromagnetic pump pressure measurement apparatus.

introduction of the cover gas. Argon gas was used for pressurization. Two MKS model 221 differential capacitance manometers were used to monitor the pressure in each reservoir. The full range of these transducers is 100 torr with a resolution of 10 mtorr. The entire system of valves, heaters, and pressurization system was controlled using a National Instruments PXI system with a LabVIEW interface.

Applied current levels ranging from 10 to 30 A were tested. Raw data from a test run are shown in figure 17(a). The figure shows a time history of pressure in the two reservoirs like that given schematically in fig. 15(b) for an applied EM pump current of 15 A. As is evident from the figure, the test procedure had to be slightly modified from the idealization outlined above. It was observed that the liquid metal had a tendency to 'stick' at low flow speeds. Consequently, the pressure in reservoir 1 did not return to its initial level in a monotonic manner. It was necessary to alternate between overpressurizing and then underpressurizing reservoir 2 to maintain liquid flow. Using this procedure, the pressure in reservoir 1 was made to oscillate about the initial pressure, with progressively decreasing amplitude. The smallest differences between the high and low values of the pressure in reservoir 2 were used to establish the bounds (uncertainty) in the pressure measurement. The pressure developed by the pump is taken as the difference between the final and initial pressure levels in reservoir 2 (ΔP_{pump} in fig. 17).

The complete data set is shown in figure 17(b). As expected, the data show that the pressure developed by the EM pump is linear with current. A linear curve fit is also shown (dashed line), which yields the calibration constant a relating the input pump current to the corresponding pump pressure produced: $P = aI$, where $a = 334 \pm 16$ Pa/A for our pump. The systematic uncertainties associated with the measurement instruments are small compared to the uncertainty inherent in the measurement procedure, and are therefore not included in the uncertainty analysis.

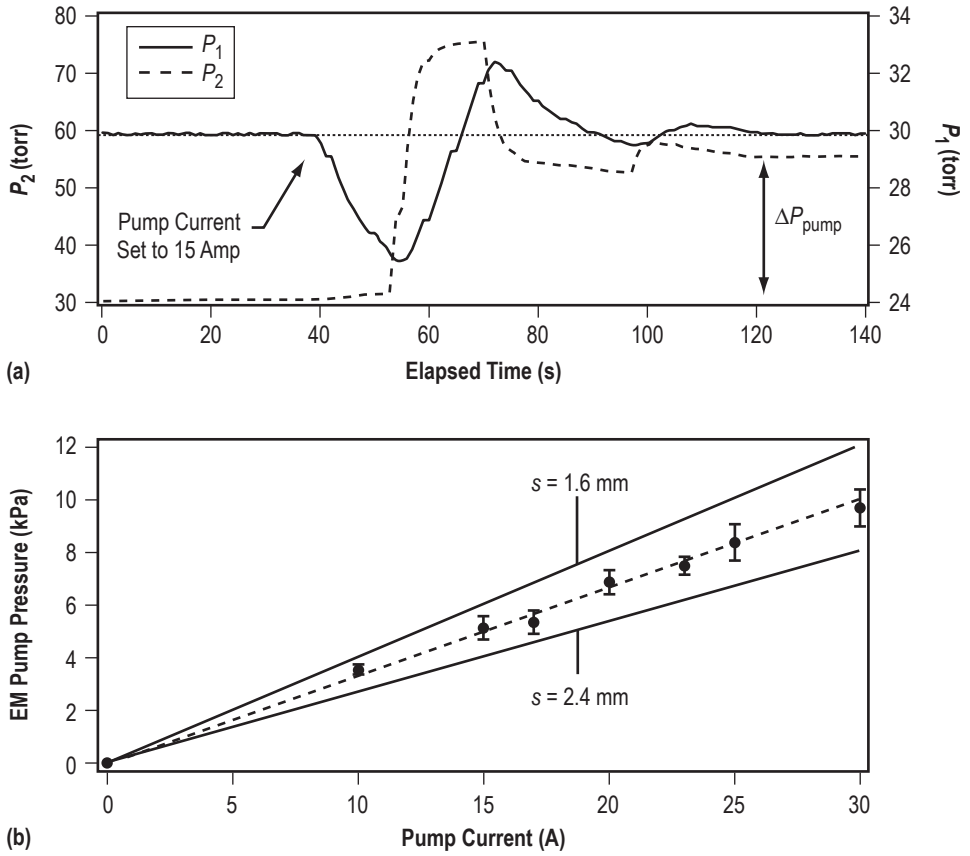

Figure 17. Experimental results for pump pressure measurement experiments: (a) Raw data showing pressure transducer output versus time (15A pump current) and (b) EM pump pressure versus current. (Solid lines are theoretical curves based on eq. (1); the dashed line represents a linear curve fit of the data.)

The measured pump performance can be compared to the theoretical predictions of eq. (1). In the bismuth pump, there is some ambiguity in the definition of the channel height (s). The pump was constructed by drilling an axial, 2.4-mm hole through which the liquid metal flows. However, the electrodes penetrate through the sides of the pump and are somewhat smaller in height (1.6 mm). The (unknown) current pattern determines the value of s, but we would expect the effective value of s to be somewhere between 1.6 and 2.4 mm in the pump. In figure 17(b), theoretical lines are plotted for each of the extreme cases. The measured data show good quantitative agreement, lying roughly midway between the two theoretical curves.

The data demonstrate that the bismuth EM pump is capable of delivering the required hydrostatic pressure ($\mathcal{O}(10^3$ Pa) for electric propulsion applications. Furthermore, the pump is seen to operate at a level consistent with the theoretical maximum performance. This implies that losses associated with stray conduction currents are negligible in the present design.

4.3 Flow Sensor Measurements

The flow sensor was operated in conjunction with a propellant vaporizer presently under development at JPL.[21] The heating pulse current output as a function of time is plotted in figure 18(a). For the initial capacitor charge of 15 V, the pulse peaked just under 80 A with a width of roughly 400 μs. While the magnitude of this output will change with the initial capacitor voltage, the waveforms will not change in shape.

Temperature measurements obtained downstream of the location where the heat pulse was introduced are presented in figure 18(b) for hot, flowing bismuth.[22] Time is measured from when the current pulse is initiated. The data presented indicate a temperature peak passing the thermocouple location ≈4 s after the heating pulse. A flow rate of 6 mg/s is estimated based upon the sensor geometry, fluid density, and hot spot time of flight. The uncertainty in this estimate of ±6% is based on the possible flow rates corresponding to the times the leading and trailing edges of the hot spot pass the thermocouple. Consistent launch and detection of such thermal features during testing was not achieved. While this test demonstrated the principle of operation, additional development work is required to produce an instrument that provides consistent, repeatable results.

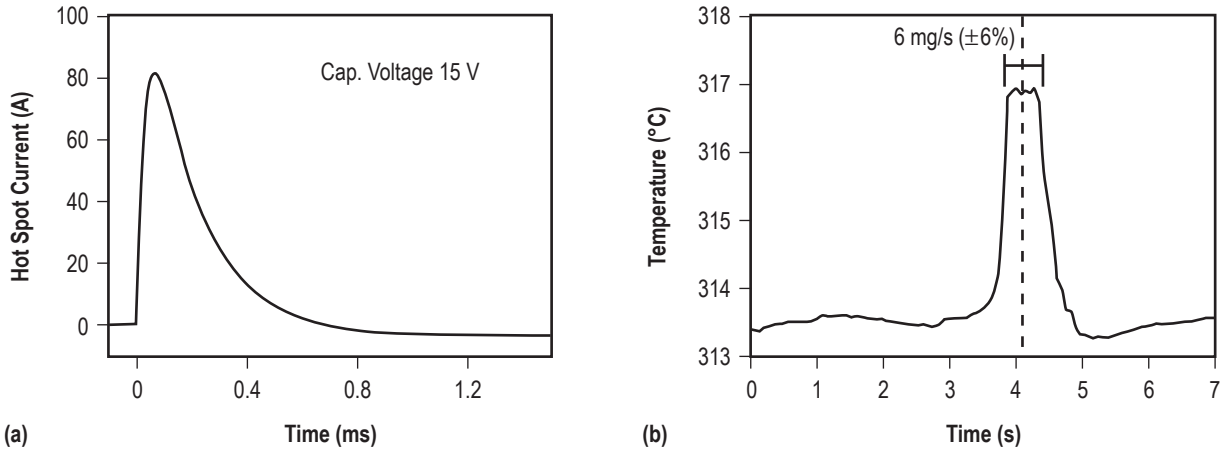

Figure 18. Flow sensor: (a) Current output of the hot spot pulse circuit for an initial charge voltage of 15 V and (b) flow sensor-measured bismuth fluid temperature as a function of time. Flow rate is estimated based upon the sensor geometry, fluid density, and hot spot time of flight.

5. PROJECT SUMMARY AND CONCLUSIONS

Two bismuth propellant feed systems were developed during the course of the VHITAL project. The first was a gas pressure-driven system that did not provide a means to measure the bismuth mass flow rate. The pressure-driven system was subsumed in the second system, which also included an EM pump and a sensor developed especially to measure the mass flow rate of bismuth. The second system also possessed a complete, self-contained electronics package capable of independently operating the entire feed system.

The following conclusions can be drawn from this work:

- The gas pressure-driven system successfully provided liquid bismuth to a propellant vaporizer. This system is capable of pressurizing the liquid bismuth over a nearly continuous range from zero to 200 torr using off-the-shelf components.

- High-temperature material compatibility was a driving design requirement for the bismuth EM pump and flow sensor. Macor was chosen for the insulating body material to minimize shunt conduction current losses. Posttest inspection after exposure to hot, flowing bismuth revealed no degradation in either component.

- The EM pump produced a hydrodynamic pressure in the liquid metal of 10 kPa when operating at 30 A. A measure of pump pressure as a function of input current showed good quantitative agreement with the theoretical pump output.

- The flow sensing technique employed by the hot spot flow sensor was successfully demonstrated using hot, flowing bismuth during operation of the full-feed system in conjunction with a propellant vaporizer. A flow rate of 6 mg/s with an uncertainty of $\pm 6\%$ was estimated based on data from the flow sensor. The flow rate measurements were not repeatable, possibly due to pressure fluctuations in other system components. Additional experiments of the integrated system are required but preliminary results are encouraging.

- A cRIO real-time controller, coupled with a remote computer/user interface through a fiber optic network converter, was used to control all feed system electronics and simultaneously perform all data acquisition. A demonstration of the entire system—power supplies, pulse circuit, data acquisition—demonstrated the ability to control and monitor the feed system using a remote computer interface.

REFERENCES

1. Tverdokhlebov, S.O.; Semenkin, A.V.; and Polk, J.E.: "Bismuth Propellant Option for Very High Power TAL Thruster," *AIAA Paper 2002–348*, 40th AIAA Aerospace Sciences Meeting and Exhibit, Reno, NV, January 14–17, 2002.

2. Sengupta, A.; Marrese-Reading, C.; Cappelli, M.; et al.: "An Overview of the VHITAL Program: A Two-stage Bismuth Fed Very High Specific Impulse Thruster With Anode Layer," *IEPC–2005–238*, 29th International Electric Propulsion Conference, Princeton, NJ, October 31–November 4, 2005.

3. Barnes, A.H.: "Direct-current Electromagnetic Pumps," *Nucleonics*, Vol. 11(1), p. 16, January 1953.

4. Markusic, T.E.; Polzin, K.A.; Stanojev, B.J.; et al.: "Liquid Metal Flow Sensors for Electric Propulsion," 53rd JANNAF Propulsion Meeting/2nd Liquid Propulsion/1st Spacecraft Propulsion Subcommittee Joint Meeting, Monterey, CA, December 2005.

5. Polzin, K.A.; and Choueiri, E.Y.: "A Similarity Parameter for Capillary Flows," *J. Phys. D: Appl. Phys.*, Vol. 36, p. 3156, December 2003.

6. Forrester, A.T.; and Barcatta, F.A.: "Surface Tension Storage and Feed Systems for Ion Engines," *J. Spacecraft Rockets*, Vol. 3(7), p. 1080, July 1966.

7. Trump, G.E.; Forrester, A.T.; and Barcatta, F.A.: "Surface Tension Storage and Feed Systems for Ion Engines," *AIAA Paper 1966–249*, 5th AIAA Electric Propulsion Conference, San Diego, CA, March 7–9, 1966.

8. Collett, C.R.; Dulgeroff, C.R.; and Simpkins, J.M.: "Cesium Microthruster System," *AIAA Paper 1969–292*, 7th AIAA Electric Propulsion Conference, Williamsburg, VA, March 3–5, 1969.

9. Marcuccio, S.; Genovese, A.; and Andrenucci, M.: "Experimental Performance of Field Emission Microthrusters," *J. Propul. Power*, Vol. 14(5), p. 774, September–October 1998.

10. Tajmar, M.; Genovese, A.; and Steiger, W.: "Indium Field Emission Electric Propulsion Microthruster Experimental Characterization," *J. Propul. Power*, Vol. 2(2), p. 211, March–April 2004.

11. King, H.J.; Molitor, J.H.; and Kami, S.: "System Concepts for a Liquid Mercury Cathode Thruster," *AIAA Paper 1967–699*, AIAA Electric Propulsion and Plasmadynamics Conference, Colorado Springs, CO, September 11–13, 1967.

12. Hyman, J., Jr.; Bayless, J.R.; Schnelker, D.E.; et al.: "Development of a Liquid-Mercury Cathode Thruster System," *J. Spacecraft Rockets*, Vol. 8(7), p. 717, July 1971.

13. Holcomb, L.B.; and Womack, J.R.: "Design of a Mercury Propellant Storage and Distribution Assembly," *AIAA Paper 1973–1119*, 10th AIAA Electric Propulsion Conference, Lake Tahoe, NV, October 31–November 2, 1973.

14. Bennett, S.; John, R.R.; Enos, G.; and Tuchman, A.: "Experimental Investigation of the MPD Arcjet," *AIAA Paper 1966–239*, 5th AIAA Electric Propulsion Conference, San Diego, CA, March 7–9, 1966.

15. Connolly, D.J.; Sovie, R.J.; Michels, C.J.; and Burkhart, J.A.: "Low Environmental Pressure MPD Arc Tests," *AIAA J.*, Vol. 6(7), p. 1271, July 1968.

16. Kodys, A.D.; Emsellem, G.; Cassady, L.D.; et al., "Lithium Mass Flow Control for High Power Lorentz Force Accelerators," *AIP Conference Proceedings*, Vol. 552, p. 908, February 2001.

17. Cassady, L.D.; Kodys, A.D.; and Choueiri, E.Y.: "A Thrust Stand for High-power Steady-state Plasma Thrusters," *AIAA Paper 2002–4118*, 38th AIAA/ASME/SAE/ASEE Joint Propulsion Conference and Exhibit, Indianapolis, IN, July 7–10, 2002.

18. Choueiri, E.Y.; Chiravalle, V.; Miller, G.E.; et al.: "Lorentz Force Accelerator With an Open-ended Lithium Heat Pipe," *AIAA Paper 1996–2737*, 32nd ASME/SAE/ASEE Joint Propulsion Conference and Exhibit, Lake Buena Vista, FL, July 1–3, 1996.

19. Schmidt, G.L.: "SNAP10A Test Program," Air Force Weapons Laboratory Report, *SP-100-XT-0002*, September 1988.

20. Markusic, T.E.; Polzin, K.A.; and Dehoyos, A.: "Electromagnetic Pumps for Conductive-Propellant Feed Systems," *IEPC–2005–295*, 29th International Electric Propulsion Conference, Princeton, NJ, October 31–November 4, 2005.

21. Marrese-Reading, C.; Swindlehurst, R.; Owens, R.; et al.: "The Development of a Bismuth Feed System for the Very High I_{sp} Thruster with Anode Layer (VHITAL) Program," *AIAA Paper 2006-4635*, 42nd AIAA/ASME/SAE/ASEE Joint Propulsion Conference, Sacramento, CA, July 9–12, 2006.

22. Polzin, K.A.; Markusic, T.E.; Stanojev, B.J.; and Marrese-Reading, C.: "Integrated Liquid Bismuth Propellant Feed System," *AIAA Paper 2006–4636*, 42nd AIAA/ASME/SAE/ASEE Joint Propulsion Conference, Sacramento, CA, July 9–12, 2006.

REPORT DOCUMENTATION PAGE

Form Approved
OMB No. 0704-0188

1. AGENCY USE ONLY *(Leave Blank)*	2. REPORT DATE	3. REPORT TYPE AND DATES COVERED
	May 2007	Technical Memorandum

4. TITLE AND SUBTITLE

Liquid Bismuth Propellant Management System for the Very High Specific Impulse Thruster With Anode Layer

5. FUNDING NUMBERS

6. AUTHORS

K.A. Polzin, T.E. Markusic, and B.J. Stanojev*

7. PERFORMING ORGANIZATION NAME(S) AND ADDRESS(ES)

George C. Marshall Space Flight Center
Marshall Space Flight Center, AL 35812

8. PERFORMING ORGANIZATION REPORT NUMBER

M–1187

9. SPONSORING/MONITORING AGENCY NAME(S) AND ADDRESS(ES)

National Aeronautics and Space Administration
Washington, DC 20546–0001

10. SPONSORING/MONITORING AGENCY REPORT NUMBER

NASA/TM—2007–214958

11. SUPPLEMENTARY NOTES

Prepared by the Propulsion Systems Department. Engineering Directorate
*WFI Government Services, Inc., 401 Wynn Drive, Huntsville, AL 35805

12a. DISTRIBUTION/AVAILABILITY STATEMENT

Unclassified-Unlimited
Subject Category 20
Availability: NASA CASI 301–621–0390

12b. DISTRIBUTION CODE

13. ABSTRACT *(Maximum 200 words)*

Two prototype bismuth propellant feed systems were constructed and operated in conjunction with a propellant vaporizer. One system provided bismuth to a vaporizer using gas pressurization but did not include a means to measure the flow rate. The second system incorporated an electromagnetic pump to provide fine control of the hydrostatic pressure and a new type of in-line flow sensor that was developed for accurate, real-time measurement of the mass flow rate. High-temperature material compatibility was a driving design requirement for the pump and flow sensor, leading to the selection of Macor® for the main body of both components. Posttest inspections of both components revealed no degradation of the material. The gas pressurization system demonstrated continuous pressure control over a range from zero to 200 torr. In separate proof-of-concept experiments, the electromagnetic pump produced a linear pressure rise as a function of current that compared favorably with theoretical pump pressure predictions, producing a pressure rise of 10 kPa at 30 A. Preliminary flow sensor operation indicated a bismuth flow rate of 6 mg/s with an uncertainty of ±6%. An electronics suite containing a real-time controller was successfully used to control the entire system, simultaneously monitoring all power supplies and performing data acquisition duties.

14. SUBJECT TERMS

bismuth Hall thruster, propellent feed system, propellant control system, electromagnetic pump, bismuth flow sensor

15. NUMBER OF PAGES

36

16. PRICE CODE

17. SECURITY CLASSIFICATION OF REPORT	18. SECURITY CLASSIFICATION OF THIS PAGE	19. SECURITY CLASSIFICATION OF ABSTRACT	20. LIMITATION OF ABSTRACT
Unclassified	Unclassified	Unclassified	Unlimited

National Aeronautics and
Space Administration
IS20
George C. Marshall Space Flight Center
Marshall Space Flight Center, Alabama
35812